AMERICAN SOCIETY FOR MICROBIOLOGY | Antimicrobial Agents and Chemotherapy®

CLINICAL THERAPEUTICS

Population Pharmacokinetic-Pharmacodynamic Model of Oxfendazole in Healthy Adults in a Multiple Ascending Dose and Food Effect Study and Target Attainment Analysis

Thanh Bach,[a] Gregory A. Deye,[b] Ellen E. Codd,[c,d] John Horton,[d,e] Patricia Winokur,[f] Guohua An[a]

[a]Division of Pharmaceutics and Translational Therapeutics, College of Pharmacy, University of Iowa, Iowa City, Iowa, USA
[b]Division of Microbiology and Infectious Diseases, National Institute of Allergy and Infectious Diseases, Bethesda, Maryland, USA
[c]Codd Consulting, LLC, Blue Bell, Pennsylvania, USA
[d]Oxfendazole Development Group, Blue Bell, Pennsylvania, USA
[e]Tropical Projects, Hitchin, United Kingdom
[f]Division of Infectious Diseases, Carver College of Medicine, University of Iowa, Iowa City, Iowa, USA

ABSTRACT Oxfendazole is a potent veterinary antiparasitic drug undergoing development for human use to treat multiple parasitic infections. Results from two recently completed phase I clinical trials conducted in healthy adults showed that the pharmacokinetics of oxfendazole is nonlinear, affected by food, and, after the administration of repeated doses, appeared to mildly affect hemoglobin concentrations. To facilitate oxfendazole dose optimization for its use in patient populations, the relationship among oxfendazole dose, pharmacokinetics, and hemoglobin concentration was quantitatively characterized using population pharmacokinetic-pharmacodynamic modeling. In fasting subjects, oxfendazole pharmacokinetics was well described by a one-compartment model with first-order absorption and elimination. The change in oxfendazole pharmacokinetics when administered following a fatty meal was captured by an absorption model with one transit compartment and increased bioavailability. The effect of oxfendazole exposure on hemoglobin concentration in healthy adults was characterized by a life span indirect response model in which oxfendazole has positive but minor inhibitory effect on red blood cell synthesis. Further simulation indicated that oxfendazole has a low risk of posing a safety concern regarding hemoglobin concentration, even at a high oxfendazole dose of 60 mg/kg of body weight once daily. The final model was further used to perform comprehensive target attainment simulations for whipworm infection and filariasis at various dose regimens and target attainment criteria. The results of our modeling work, when adopted appropriately, have the potential to greatly facilitate oxfendazole dose regimen optimization in patient populations with different types of parasitic infections.

KEYWORDS benzimidazole, mathematical modeling, model-informed drug development, oxfendazole, population PK/PD modeling, target attainment analysis

Neglected tropical diseases are a diverse set of infections caused by bacteria, viruses, protozoa, and metazoa that affect more than 1.5 billion people worldwide (1). Even though some neglected tropical diseases have been effectively controlled and almost eradicated, there remain multiple difficult-to-treat infections, which include neurocysticercosis, trichuriasis, echinococcosis, fascioliasis, and filariasis. Although these diseases are currently treated by the benzimidazole anthelmintic drugs albendazole, mebendazole, or triclabendazole, these treatments are not optimal due to their low efficacy (2–5), drug resistance (6), and/or unfavorable pharmacokinetics (e.g., short and greatly variable half-life) (7–9).

Oxfendazole is a potent benzimidazole anthelmintic marketed to treat lungworm and enteric helminths in animals (10). A single oral low dose of oxfendazole effectively reduced

Copyright © 2022 American Society for Microbiology. All Rights Reserved.

Address correspondence to Guohua An, guohua-an@uiowa.edu.

Received 19 July 2021
Returned for modification 1 September 2021
Accepted 29 September 2021
Accepted manuscript posted online 4 October 2021
Published 18 January 2022

worm burden in *Trichuris suis*-infected pigs (11, 12), a surrogate model of human whipworm infection. In filaria-infected mice, orally or subcutaneously administered oxfendazole demonstrated up to 100% macrofilaricidal efficacy at a dosing regimen of 25 mg/kg of body weight daily for 5 days (13). The preclinical efficacy of oxfendazole in the treatment of neurocysticercosis, echinococcosis, and fascioliasis was presented in detail in a recent review (14). These results suggest that oxfendazole is a potential candidate for the treatment of multiple parasitic infections in humans. This is further supported by the favorable safety (10, 15) and pharmacokinetic profiles of oxfendazole in preclinical species. Oxfendazole exposure and half-life were greater than or comparable to those of albendazole and mebendazole in dogs (16), sheep (17), pigs (18, 19), and rats (15, 20).

Previously, the safety, tolerability, and pharmacokinetics of oxfendazole and its metabolites in healthy adults were evaluated following oral administration of single ascending oxfendazole doses between 0.5 and 60 mg/kg (21). In that study, oxfendazole was the major moiety detected in plasma, followed by oxfendazole sulfone and fenbendazole (21). The same relative systemic exposure to parent drug and metabolites was observed in pigs (22), supporting their use as an appropriate preclinical model for oxfendazole toxicity and efficacy. In a disposition study of oxfendazole in *T. suis*-infected pigs, the oxfendazole concentration in whipworm tissue was highly correlated with the drug's concentration in pig plasma (22), suggesting that plasma is a significant route for oxfendazole access to whipworm. Further, in humans, the dose-normalized exposure of oxfendazole was 27 times higher than that of albendazole and 538 times higher than that of mebendazole (23–25). Taken together, these data suggest that oxfendazole has an advantageous pharmacokinetic profile compared to those of albendazole and mebendazole for the treatment of whipworm infection in humans.

Given the encouraging results from the single ascending dose oxfendazole clinical trial, we recently completed and published the results of the second clinical trial assessing oxfendazole safety, tolerability, and pharmacokinetics in healthy adults following the administration of multiple ascending doses from 3 to 15 mg/kg (ClinicalTrials.gov registration no. NCT03035760) (23). In healthy adults, oxfendazole absorption was rapid, with a time to maximum concentration (T_{max}) of ~2 h. Oxfendazole elimination half-life (9.21 to 11.8 h) was consistent across dose groups and, following the administration of multiple doses at 24-h intervals, oxfendazole plasma levels reached steady state on day 3 with little accumulation (accumulation ratio, 0.970 to 1.27). Oxfendazole exhibited substantial nonlinear pharmacokinetics with a less than dose-proportional increase in plasma exposure with escalating doses, most likely due to oxfendazole's low solubility, which caused a decrease in bioavailability with increasing doses. When oxfendazole was administered following a high-fat breakfast, oxfendazole's peak concentration (C_{max}) increased 1.49 times and the T_{max} increased by 6.88 h compared to those in the fasted state. A mild decrease in hemoglobin (Hb) concentration with increasing oxfendazole dose was observed, although hemoglobin concentrations remained within the normal range for most subjects.

Because oxfendazole concentration in plasma is related to both efficacy and potential hematologic effects, an insight into the correlation between oxfendazole dose and exposure is important for dose optimization. However, oxfendazole nonlinear pharmacokinetics makes correlation of oxfendazole dose to exposure difficult. Therefore, in this study, we performed a secondary analysis of oxfendazole pharmacokinetics and its effect on hemoglobin concentration using the population pharmacokinetic-pharmacodynamic (popPK/PD) modeling approach. Because a popPK/PD model describes the underlying system, once developed, the model can be used to predict oxfendazole PK/PD with new dosing regimens that have not been evaluated in humans and be applied to other efficacy endpoints. Thus, we have applied the developed popPK/PD model of oxfendazole to predict (i) the change in hemoglobin concentration following multiple ascending doses from 3 to 60 mg/kg and (ii) the probability of target attainment of oxfendazole in treating whipworm infection and filariasis in humans.

RESULTS

Population pharmacokinetic-pharmacodynamic model. (i) Structural model. ***(a) Pharmacokinetic model.*** Structural pharmacokinetic models for oxfendazole in the fasted state and fed state are presented in Fig. 1A and B, respectively. The prolonged

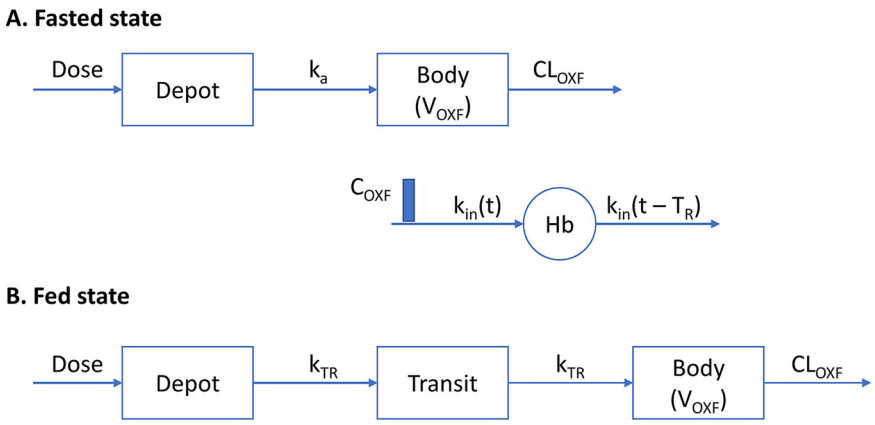

FIG 1 (A) Structural PK/PD model for oxfendazole and its effect on hemoglobin concentration following multiple ascending doses and following a single dose in the fasted state. (B) Structural PK model for oxfendazole following single oral dose in the fed state.

absorption of oxfendazole in the fed state was best captured by an absorption model with 1 transit compartment.

(b) Pharmacodynamic model. Two models were examined to characterize the decrease in hemoglobin concentration with multiple ascending oxfendazole doses: (i) the basic indirect response model with inhibition of hemoglobin synthesis and (ii) the life span indirect response model with inhibition of red blood cell synthesis. The two models performed similarly well based on Akaike information criterion (AIC), parameter feasibility and precision, and goodness-of-fit plots. The more mechanistic life span model (Fig. 1A) was chosen as the final structural pharmacodynamic model because it is known that red blood cells are cleared after an average of 120 days in adults (i.e., they have relatively consistent life span). In this model, oxfendazole's inhibitory effect on hemoglobin synthesis was linearly correlated with oxfendazole concentration in plasma.

(ii) Stochastic model. Interindividual and interoccasion variability of all pharmacokinetic parameters were investigated. Interindividual variability in transit rate constant (k_{TR}), absorption rate constant (k_a), oxfendazole apparent volume of distribution (V_{OXF}), oxfendazole apparent clearance (CL_{OXF}), and hemoglobin synthesis rate constant (k_{in}), and interoccasion variability in V_{OXF} and CL_{OXF} were significant.

(iii) Covariate model. None of the evaluated covariates had significant impact on oxfendazole pharmacokinetics. Sex significantly affected k_{in}, with k_{in} in females being 91.3% (95% confidence interval, 90.8 to 91.8%) of that in males (Table 1).

(iv) Model evaluation. Model evaluation based on goodness-of-fit plots indicated no systemic bias in terms of oxfendazole plasma concentration (see Fig. S1 in the supplemental material) or hemoglobin concentration (Fig. S2). Figure 2 presents the time course of population-predicted oxfendazole concentrations versus the mean observed oxfendazole concentrations following the administration of multiple ascending doses (upper) or a single dose in fasted and fed states (lower). The change in population-predicted hemoglobin concentration versus change in observed hemoglobin concentration after the administration of multiple oxfendazole doses is presented in Fig. 3. Overall, there was good agreement between model-predicted and observed data under all dosing regimens and conditions, indicating that the model was sufficient at capturing oxfendazole PK/PD.

Final estimates of model parameters are summarized in Table 1. Percent relative standard error (%RSE) was $<$30% for all PK/PD parameters, suggesting that all PK/PD parameters were estimated with good precision. The estimated variance of interindividual variability in k_a, k_{TR}, and V_{OXF} had %RSE of more than 50%. However, removal of these interindividual variability terms negatively impacted model performance. Condition numbers (ratio of the highest to the lowest eigenvalue) were 269.3 for the final pharmacokinetic model and 1.6 for the final pharmacodynamic model. Condition numbers being less than 1,000 indicate that the model is not ill-conditioned or overparameterized.

TABLE 1 Final estimates of oxfendazole population pharmacokinetic-pharmacodynamic model parameters

Parameter	Definition	Estimate	% RSE[b]	% shrinkage
θ_1	A parameter in calculation of bioavailability (F)[a]	−0.646	11.2	
θ_2 (mg)	A parameter in calculation of bioavailability (F)	209.25 FIX		
F_{fed}/F_{fast}	Ratio of bioavailability in fed state to bioavailability in fasted state	2.08	12.4	
k_{TR} (h^{-1})	First-order transit rate constant in fed state	0.412	14.7	
k_a (h^{-1})	First-order absorption rate constant in fasted state	1.2	7.1	
V_{OXF} (liter)	Oxfendazole apparent vol of distribution	34.5	8.0	
CL_{OXF} (liter/h)	Oxfendazole apparent clearance	2.57	8.6	
θ (ml/ng)	Linear coefficient for the inhibitory effect of oxfendazole on hemoglobin synthesis	0.000458	9.5	
k_{in} (g/dl/h)	Zero-order rate constant of hemoglobin synthesis in male	0.00509	1.6	
T_R (h)	Red blood cell lifespan	2,880 FIX		
θ_{sex}	The ratio of k_{in} in female to k_{in} in male	0.913	2.7	
k_{TR} IIV (CV%)	Interindividual variability in k_{TR}	47.4	52.0	44
k_a IIV (CV%)	Interindividual variability in k_a	28.6	90.6	31
V_{OXF} IIV (CV%)	Interindividual variability in V_{OXF}	20.1	59.9	17
CL_{OXF} IIV (CV%)	Interindividual variability in CL_{OXF}	37.3	33.2	7
$\rho_{V\ IIV CL\ IIV}$	Correlation of V_{OXF} IIV and CL_{OXF} IIV	0.771	10.9	
V_{OXF} IOV (CV%)	Interoccasion variability in V_{OXF}	24.1	34.6	21
CL_{OXF} IOV (CV%)	Interoccasion variability in CL_{OXF}	32.1	52.6	26
$\rho_{V\ IOV CL\ IOV}$	Correlation of V_{OXF} IOV and CL_{OXF} IOV	0.887	15.2	
k_{in} IIV (CV%)	Interindividual variability in k_{in}	60.8	35.8	20
$\sigma^2_{OXF,prop}$	Variance of oxfendazole proportional residual error	0.0616	10.4	13
$\sigma^2_{OXF,add}$	Variance of oxfendazole additive residual error	0.261	69.0	13
$\sigma^2_{Hb,prop}$	Variance of hemoglobin proportional residual error	0.000600	14.4	10

[a]$\text{Log}(F) = \theta_1 \log(\text{dose}/\theta_2) + (\text{fast}-1)\log(F_{fed}/F_{fast})$, fast = 0 in fasted state, fast = 1 in fed state.
[b]% RSE = standard error × 100/parameter estimate.

Model predictive performance was evaluated using prediction-corrected visual predictive check as presented in Fig. 4 for all dose groups and in Fig. S4 and S5 for each dose group. Based on these figures, the observed 5th, 50th, and 95th percentiles were within the 95% confidence interval of the respective simulated percentiles, suggesting that the final popPK/PD model for oxfendazole and its effect on hemoglobin concentrations had good predictive performance.

Simulation. (i) Simulation of exposure-response on safety. To investigate the maximal decrease in hemoglobin concentrations following the administration of multiple ascending oxfendazole doses, hemoglobin concentrations in healthy subjects were simulated following the administration of multiple ascending oxfendazole doses at 3, 7.5, 15, 30, and 60 mg/kg once daily for 5 days and compared to the normal range and toxicity grade 1 to 3 ranges of hemoglobin in adults. Among the simulated doses, 3 to 15 mg/kg were evaluated in oxfendazole multiple ascending dose trials, and 30- to 60-mg/kg doses were evaluated in the single ascending dose trial. The simulation did not include doses higher than 60 mg/kg because oxfendazole exposure is saturated due to dose-limited bioavailability (21).

Simulated hemoglobin concentrations following the administration of multiple ascending doses of oxfendazole to males and females are presented in Fig. 5. According to the life span model, baseline hemoglobin concentration is a product of T_R and k_{in}. Because interindividual variability in T_R was fixed to 0, the variability in simulated hemoglobin concentration at baseline was due to interindividual variability of k_{in} (Table 1). Although the magnitude of the decrease in hemoglobin concentration increased with ascending oxfendazole doses (Fig. 5), the median hemoglobin concentration remained in the normal range at all dose levels.

(ii) Simulation of exposure-response on efficacy. ***(a) Target attainment analysis for whipworm infection (approach 1).*** In the first approach to target attainment analysis for whipworm infection, a 50% infective concentration (IC_{50}) of 480 ng/ml was estimated as the concentration of oxfendazole in plasma that resulted in 50% inhibition of tubulin assembly in whipworm. (Detailed derivation of this concentration is described in Materials and Methods.)

If 100% of adult whipworms are eliminated from the body when peak concentration at steady state ($C_{max,ss}$) is equal to the IC_{50}, 100% of the patients would be cured even at the lowest simulated dose of 0.5 mg/kg (Fig. 6). If targeted $C_{max,ss} = 5 \times IC_{50}$, 90% target attainment

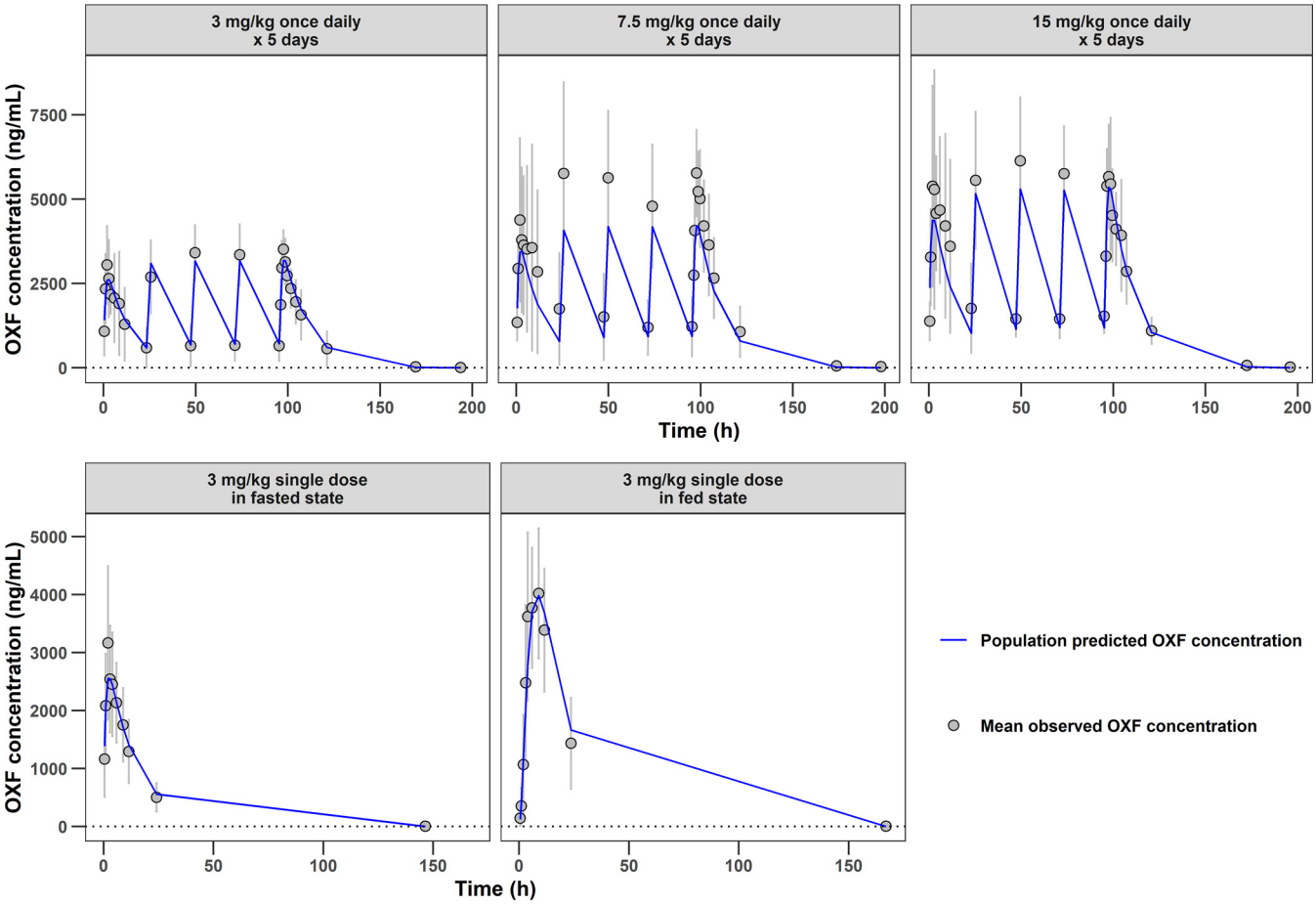

FIG 2 Time course of population predicted oxfendazole concentration and observed oxfendazole concentration following multiple ascending doses at 3, 7.5, and 15 mg/kg once daily for 5 days (upper) and following a single 3-mg/kg dose in fasted state and fed state (lower). Observed concentrations are presented as mean ± standard deviation for each group (N = 8 for multiple ascending doses evaluation, N = 12 for food effect evaluation).

was achieved at doses of ≥7.5 mg/kg. At targeted $C_{max,ss}$ = 10 × IC_{50}, 90% target attainment was achieved at doses of ≥50 mg/kg. At targeted $C_{max,ss}$ ≥ 15 × IC_{50}, probability of target attainment dropped below 70% at all doses, 0.5 to 60 mg/kg.

Because whipworm elimination might depend on how long the worm is exposed to oxfendazole, target attainment analysis was additionally performed based on $T_{>IC50}$ (i.e., the percent time of a dosing interval [24 h] at steady state during which oxfendazole concentration is above the IC_{50}), and the results are summarized in Table 2. According to Table 2, if maintenance of oxfendazole concentration above IC_{50} ($T_{>IC50}$ = 100%) is required for complete whipworm elimination, 90% of the patients would be completely cured at oxfendazole doses of 30 to 60 mg/kg. If $T_{>IC50}$ ≥ 80% is taken as the criteria for complete deworming, 90% target attainment is reached at doses above 5 mg/kg. At $T_{>IC50}$ ≥ 60%, 90% target attainment is achievable at doses above 4 mg/kg. At $T_{>IC50}$ ≥ 40%, 90% target attainment is possible at doses as low as 1 mg/kg.

(b) Target attainment analysis for whipworm infection (approach 2). In the second approach to target attainment analysis for whipworm infection, an IC_{50} of 5,290 ng/ml was estimated as the concentration of oxfendazole in plasma at which 50% of adult whipworms are killed. (Rationales for the proposed IC_{50} are discussed in Materials and Methods.)

Assuming that whipworm elimination depends on oxfendazole $C_{max,ss}$, to achieve 100% cure rate, $C_{max,ss}$ must be higher than an IC_{50} of 5,290 ng/ml. According to Fig. 7, the probability of target attainment was less than 90% for all doses other than the 60-mg/kg dose. Table 3 presents the probability of target attainment based on $T_{>IC50}$. For $T_{>IC50}$ ≥ 40%, probability of target attainment is less than 50% at all doses (0.5 to 60 mg/kg).

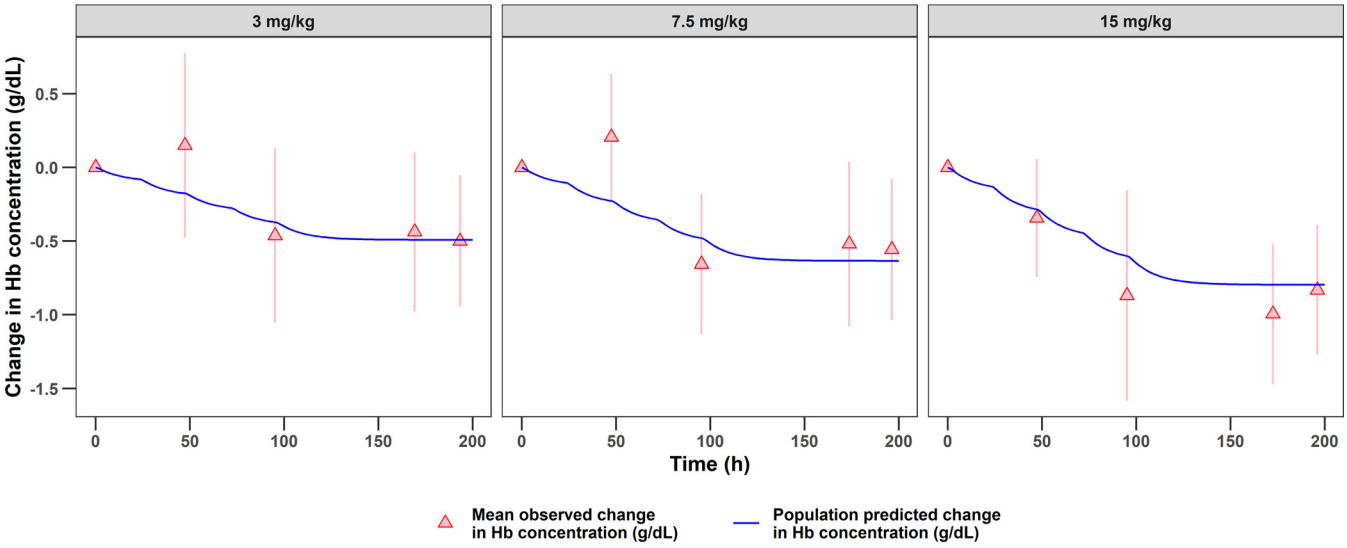

FIG 3 Time course of the change in population predicted hemoglobin concentration and change in observed hemoglobin concentration from baseline following multiple ascending doses at 3, 7.5, and 15 mg/kg once daily for 5 days. Observed concentrations are presented as mean ± standard deviation for each dose group ($N = 8$).

(c) Target attainment analysis for filariasis. Based on a mouse model of filariasis, the macrofilaricidal effect (i.e., killing of adult worms) of oxfendazole is driven by the maintenance of the minimal efficacious concentration (MEC) of 100 ng/ml in plasma. To account for uncertainty extrapolating exposure-response data from mouse to human, target attainment analysis was performed at different MEC values, ranging from 100 to 4,000 ng/ml. The mean simulated concentration-time profile of oxfendazole in human plasma following multiple ascending doses (0.5 to 60 mg/kg once daily for 5 days) compared to different MEC levels is presented in Fig. 8A, and the probability of target attainment at different MEC values and dosing regimens is presented in Fig. 8B. According to Fig. 8A, the mean concentrations of oxfendazole at all doses are above the MEC throughout the dosing interval given MEC of 100 and 200 ng/ml. Correspondingly, Fig. 8B demonstrates that the probability of target attainment at MEC of 100 ng/ml is in the range of 90 to 100% under all dosing regimens. At MEC of 200 ng/ml, probability of target attainment is ≥90% at doses of at least 3 mg/kg. At MEC of 500 ng/ml, 90% target attainment is achieved only at doses of 30 mg/kg and above. At MEC of 1,000 ng/ml and 1,500 ng/ml, even the highest doses (50 and 60 mg/kg) can reach only ~75% and 50% target attainment, respectively. At MEC of ≥2,000 ng/ml, none of the simulated dose can pass 50% target attainment.

DISCUSSION

We have successfully developed a popPK/PD model characterizing oxfendazole pharmacokinetics and its effect on hemoglobin concentrations in healthy adults in a multiple ascending dose and food effect evaluation study. Oxfendazole nonlinear pharmacokinetics, attributed to oxfendazole's low solubility, was modeled with dose-dependent bioavailability. The delay in oxfendazole absorption, as well as the increase in oxfendazole exposure in the fed compared to the fasted state, were sufficiently captured by the addition of one transit compartment and increase in bioavailability, respectively. According to the model estimated parameters (Table 1), oxfendazole bioavailability reduced significantly (22 times) as the dose increased from 0.5 mg/kg to 60 mg/kg. Based on the model developed, oxfendazole's apparent volume of distribution and apparent clearance at the lowest dose were estimated to be 34.5 liters and 2.57 liters/h (Table 1), respectively, indicating that oxfendazole distribution is moderate and oxfendazole hepatic extraction is low. A previous noncompartmental analysis showed that in subjects who have consumed a fatty meal, the oxfendazole area under the concentration-time curve (AUC) increased 1.86 times, and its T_{max} was delayed by 6.88 h (23) compared to those parameters measured in fasting subjects. In agreement with the

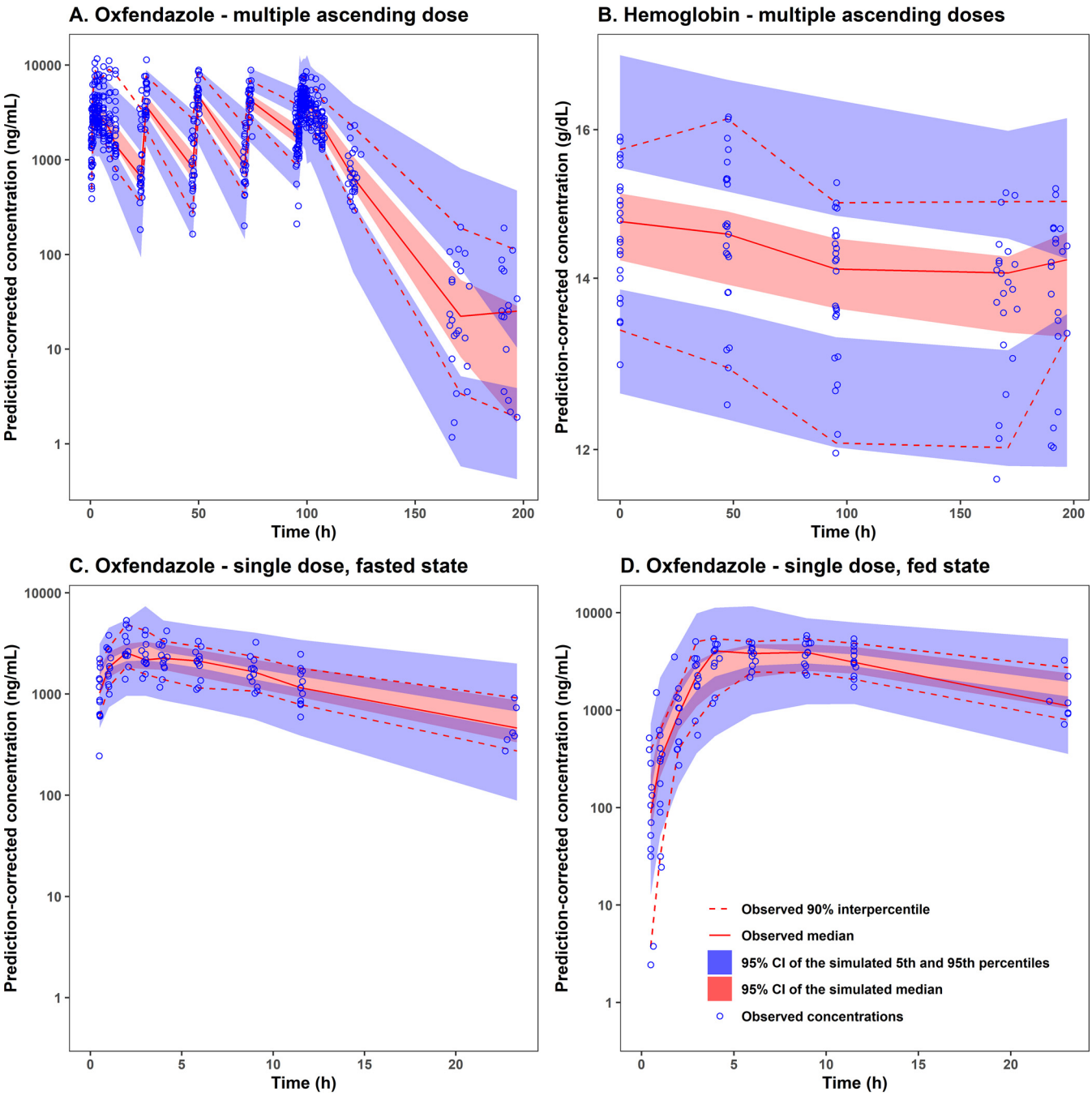

FIG 4 Prediction-corrected visual predictive check for (A) oxfendazole concentration in plasma following multiple ascending doses (3 to 15 mg/kg once daily for 5 days), (B) hemoglobin concentration in plasma following multiple ascending doses, (C) oxfendazole concentration in plasma following a single 3-mg/kg dose in fasted state, and (D) oxfendazole concentration in plasma following a single 3-mg/kg dose in fed state. CI, confidence interval.

published noncompartmental analysis results (23), our present model estimated a 2.08-fold (Table 1) increase in oxfendazole bioavailability in the fed state compared to the fasted state. In addition, in the fed state, oxfendazole absorption included one transit compartment, with the transit rate constant (0.412 h^{-1}) being much lower than the absorption rate constant of oxfendazole in the fasted state (1.2 h^{-1}) (Table 1).

The effect of oxfendazole pharmacokinetics on hemoglobin concentration following multiple doses was sufficiently characterized by a red blood cell life span model with k_{in} inhibition. Oxfendazole inhibitory effect on k_{in} followed a linear function with linear coefficient of 0.000458 (95% confidence interval, 0.000377 to 0.000539) (Table 1). At baseline,

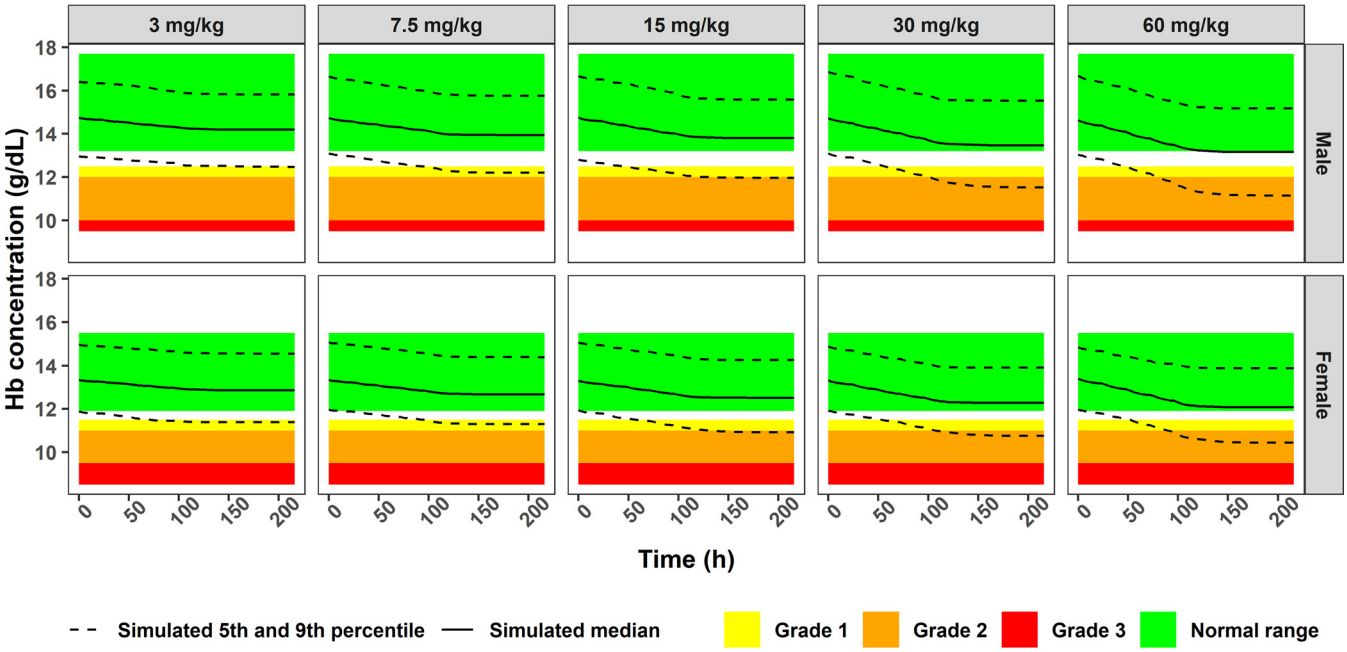

FIG 5 Simulated hemoglobin concentration in male and female subjects administered 3, 7.5, 15, 30, and 60 mg/kg oxfendazole once daily for 5 days.

hemoglobin k_{in} in males was estimated to be 0.00509 g/dl/h (equivalent to 0.122 g/dl/day). Hemoglobin k_{in} in females was 91.3% of that in males (Table 1), a result expected considering the lower normal range of hemoglobin concentration observed in females than in males (Fig. 5). Interindividual variability in oxfendazole pharmacokinetics and pharmacodynamics was low to moderate, ranging from 6% (k_{in} interindividual variability) to 47% (k_{TR} interindividual variability) (Table 1), which was expected of healthy adult subjects. A limitation of the current pharmacodynamic model is its lack of inclusion of a

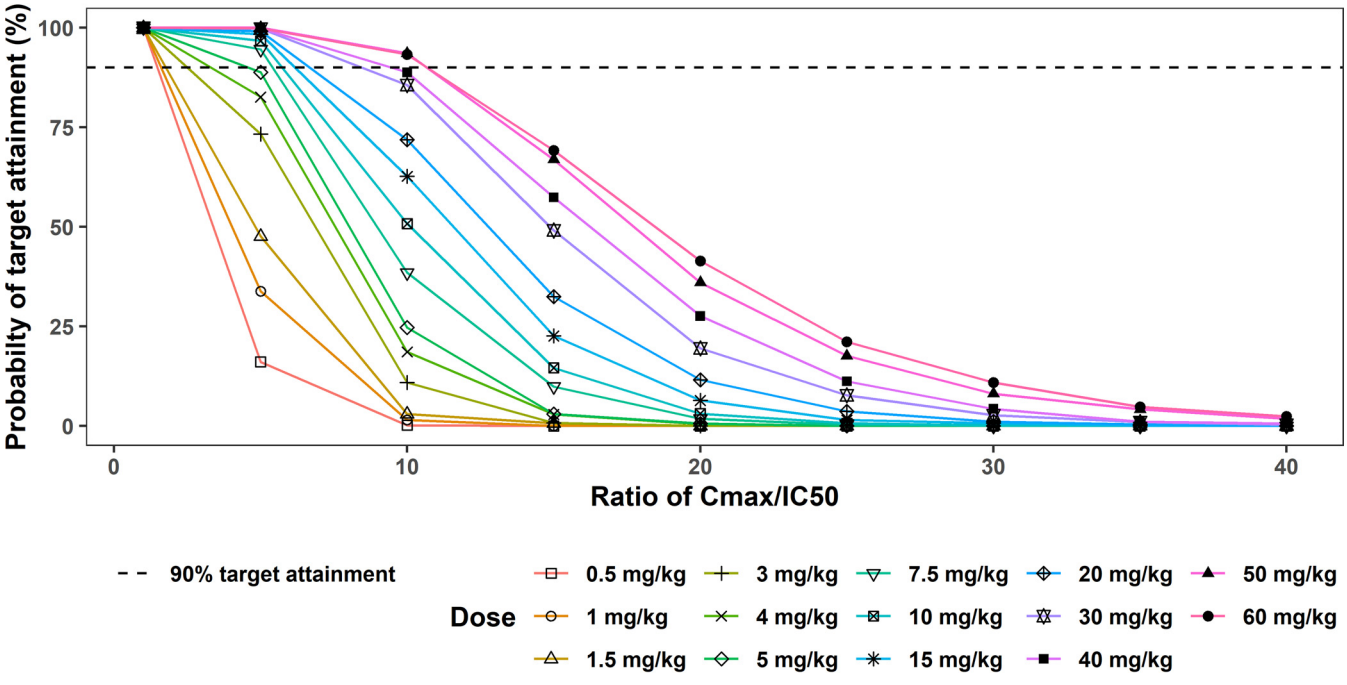

FIG 6 Probability of target attainment for whipworm infection following multiple ascending doses of oxfendazole (0.5 to 60 mg/kg once daily for 5 days) (1st approach). Probability of target attainment is the percentage of simulated subjects (1,000 subjects at each dose level) having plasma oxfendazole $C_{max,ss}$ = 1 – 40 IC_{50}. IC_{50}, 480 ng/ml.

TABLE 2 Probability of target attainment (%) for whipworm infection following multiple ascending doses of oxfendazole (0.5 to 60 mg/kg once daily for 5 days), 1st approach[a]

	$T_{>IC50}$ (%)				
Dose (mg/kg)	100	80 to <100	60 to <80	40 to <60	≤40
0.5	27.6	13.0	17.5	26.0	15.9
1	38.0	16.1	17.5	22.0	6.4
1.5	47.0	16.6	15.7	16.7	4.0
3	59.9	14.1	13.0	11.8	1.2
4	64.3	13.7	10.7	10.3	1.0
5	70.9	11.1	9.8	7.3	0.9
7.5	74.9	11.6	7.9	5.2	0.4
10	79.5	10.0	6.2	3.9	0.4
15	82.9	7.6	5.5	3.6	0.4
20	87.9	5.3	4.0	2.6	0.2
30	90.5	5.0	2.8	1.7	0.0
40	90.6	5.3	3.0	0.9	0.2
50	93.5	3.5	2.0	1.0	0.0
60	92.5	3.9	2.7	0.8	0.1

[a]Probability of target attainment is the percentage of simulated subjects (1,000 subjects at each dose level) having plasma oxfendazole concentration above IC_{50} for a certain amount of time. $T_{>IC50}$ is the percent time of a dosing interval at steady state during which oxfendazole concentration is above IC_{50} (IC_{50}, 480 ng/ml).

feedback regulation parameter, preventing its use to extrapolate to predict hemoglobin concentration after day 5.

The developed model was used for exposure-response simulations on safety and efficacy. Regarding oxfendazole safety, simulation of hemoglobin concentration following administration of multiple ascending doses of oxfendazole (3 to 60 mg/kg once daily for 5 days) demonstrated a decrease in hemoglobin concentration with increasing oxfendazole dose (Fig. 5). However, the median hemoglobin concentrations remained in the normal range, with the simulated 5th percentile reading into the grade 1 or grade 2 toxicity levels. Note the predicted value of the 5th percentile is below the normal range prior to the administration of oxfendazole.

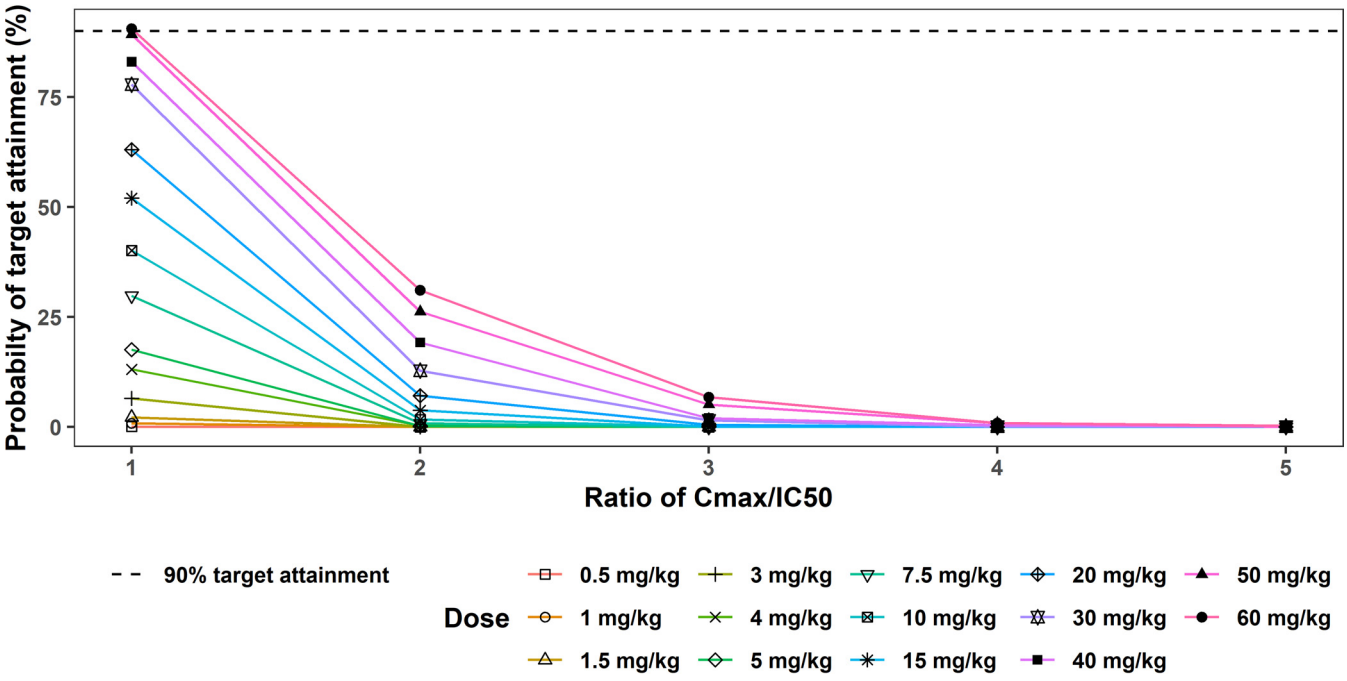

FIG 7 Probability of target attainment for whipworm infection following multiple ascending doses of oxfendazole (0.5 to 60 mg/kg once daily for 5 days) (2nd approach). Probability of target attainment is the percentage of simulated subjects (1,000 subjects at each dose level) having plasma oxfendazole $C_{max,ss}$ = 1 – 5 IC_{50}. IC_{50}, 5,290 ng/ml.

TABLE 3 Probability of target attainment (%) for whipworm infection following multiple ascending doses of oxfendazole (0.5 to 60 mg/kg once daily for 5 days), 2nd approach[a]

	$T_{>IC50}$ (%)				
Dose (mg/kg)	100	80 to <100	60 to <80	40 to <60	≤40
0.5	0.0	0.0	0.0	0.0	100
1	0.0	0.0	0.0	0.1	99.9
1.5	0.0	0.1	0.1	0.3	99.5
3	0.0	0.0	0.0	0.6	99.4
4	0.0	0.0	0.6	1.2	98.2
5	0.0	0.1	0.2	1.4	98.3
7.5	0.1	0.2	0.8	4.1	94.8
10	0.3	0.9	0.7	4.4	93.7
15	0.5	0.3	2.5	7.0	89.7
20	1.0	1.5	2.3	9.9	85.3
30	1.4	1.7	4.5	15.1	77.3
40	1.8	3.5	5.6	18.1	71.0
50	3.7	4.3	6.7	22.1	63.2
60	4.1	5.0	5.9	22.6	62.4

[a]Probability of target attainment is the percentage of simulated subjects (1,000 subjects at each dose level) having plasma oxfendazole concentration above IC_{50} for a certain amount of time. $T_{>IC50}$ is the percent time of a dosing interval at steady state during which oxfendazole concentration is above IC_{50} (IC_{50}, 5,290 ng/ml).

In terms of oxfendazole efficacy in the treatment of whipworm infection, four scenarios were explored: $C_{max,ss} \geq IC_{50}$ = 480 ng/ml, $T_{>IC50}$ (IC_{50} = 480 ng/ml), $C_{max,ss} \geq IC_{50}$ = 5,290 ng/ml, and $T_{>IC50}$ (IC_{50} = 5,290 ng/ml). The two different IC_{50} values were estimated based on different *in vitro* models with different sets of assumptions as described in Materials and Methods. $C_{max,ss} \geq IC_{50}$ = 480 ng/ml was the easiest target to achieve, with 100% of the population predicted to meet this requirement even at 0.5 mg/kg dose and 90% of the population predicted to have oxfendazole concentrations in plasma above 480 ng/ml throughout the dosing interval (i.e., $T_{>IC50}$ = 100%) with 30 to 60 mg/kg dose. In contrast, with IC_{50} = 5,290 ng/ml, 90% of the population is predicted to have $C_{max,ss} \geq IC_{50}$ = 5,290 ng/ml only at the highest dose of 60 mg/kg, and less than 5% of the population maintains an oxfendazole concentration in plasma above IC_{50} = 5,290 ng/ml throughout the dosing interval. Increasing the dose over 60 mg/kg would not improve the probability of target attainment, as oxfendazole exposure increased less than dose proportionally with increasing dose. Due to the lack of exposure-response analysis on oxfendazole efficacy in treating whipworm infection, target attainment analysis was performed using two approaches with different sets of assumptions. The two approaches estimated two IC_{50} values, which differed by 11-fold and resulted in dramatically differing probabilities of target attainment at clinically relevant doses. In addition, with the increase in dose, the change in efficacy can be very different between IC_{50} = 480 ng/ml and IC_{50} = 5,290 ng/ml. At the lower IC_{50}, increasing dose from 15 to 60 mg/kg was predicted to result in only a 10% increase in probability of target attainment, with the target being $T_{>IC50}$ = 100%. Meanwhile, at the higher IC_{50}, an increase in dose from 15 to 60 mg/kg was predicted to increase the probability of target attainment by nearly 30%, with the target being $T_{>IC50} \geq$ 40%. Thus, results of target attainment analysis should be considered with caution.

For filariasis treatment, assuming that the minimal efficacious concentration of oxfendazole in mouse (100 ng/ml) (26) and human is the same, 90% target attainment is feasible even at low dose (0.5 mg/kg).

The *in vitro* study monitoring adult *T. muris* motility in culture as an indication of live worms reported IC_{50} values of 17.7 μM, 24.2 μM, 14.3 μM, and 55.2 μM for albendazole, albendazole sulfoxide, mebendazole, and oxfendazole, respectively, indicating that oxfendazole was the least potent among the four benzimidazoles (26). Correspondingly, ED_{50} (dose at 50% worm burden reduction) values of oxfendazole and albendazole were higher than that of mebendazole in *T. muris*-infected mice. The ED_{50} values obtained were the following: oxfendazole, >300 mg/kg; albendazole, 345 mg/kg; and mebendazole, 79 mg/kg (26). The study author speculated that oxfendazole would not be any better than albendazole and

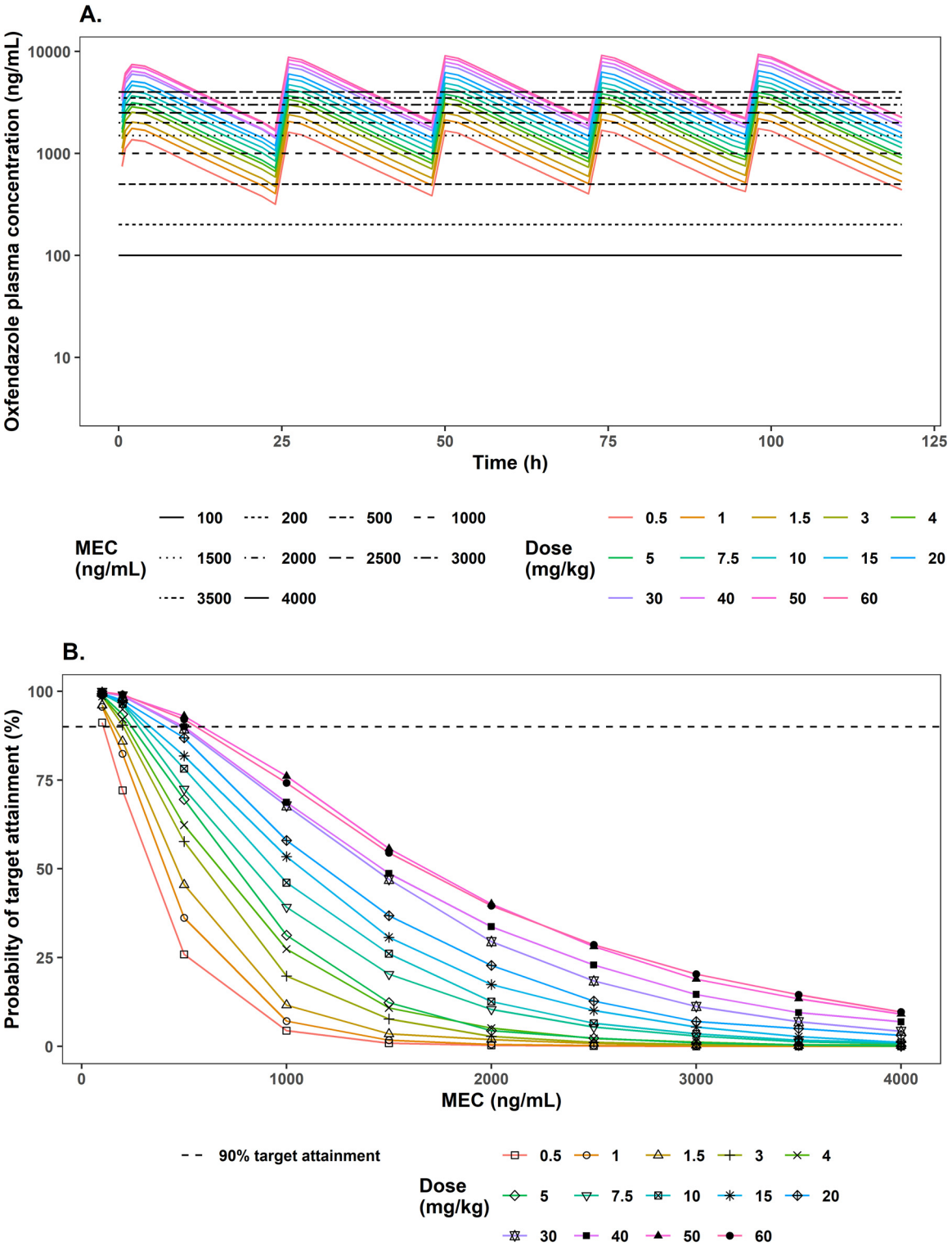

FIG 8 (A) Mean simulated concentration-time profile of oxfendazole in human plasma following multiple ascending doses of oxfendazole 0.5 to 60 mg/kg once daily for 5 days compared to different minimal efficacious concentrations (MEC) of 100 to 4,000 ng/ml. (B) Probability of target attainment for filariasis following multiple ascending doses of oxfendazole (0.5 to 60 mg/kg once daily for 5 days). Probability of target attainment is the percentage of simulated subjects (1,000 subjects at each dose level) having plasma oxfendazole concentration at steady state above MEC for 100% of the dosing interval (i.e., 24 h).

mebendazole in treating whipworm infection in humans. However, this conclusion may be premature based on the following two considerations. First, the exposure of oxfendazole in human was 27 times higher than that of albendazole sulfoxide (the major active moiety in human plasma following albendazole oral administration) and 538 times higher than that of mebendazole (23–25). Meanwhile, the oxfendazole IC_{50} determined *in vitro* was higher than that of albendazole sulfoxide and mebendazole by only 2- to 4-fold (26). Thus, the higher exposure of oxfendazole compared to albendazole sulfoxide and mebendazole could compensate for oxfendazole's lower *in vitro* potency. Second, mice might not be a good model for oxfendazole disposition and efficacy in human due to potentially different pharmacokinetic features. Oxfendazole's metabolic profile in mice is not currently available. However, according to oxfendazole pharmacokinetic studies in the rat, following oxfendazole oral administration, oxfendazole sulfone was the most abundant moiety in plasma, followed by oxfendazole and fenbendazole (27). Meanwhile, in humans, oxfendazole was the predominant moiety in plasma, followed by oxfendazole sulfone and fenbendazole (21). Considering that oxfendazole and fenbendazole are active while oxfendazole sulfone is inactive, the lack of efficacy in mice might be due to oxfendazole pharmacokinetics (i.e., low systemic exposure) rather than pharmacodynamics (i.e., *in vitro* IC_{50}).

It is worth pointing out that the current model was developed based on oxfendazole pharmacokinetics and safety data obtained from healthy adults. When oxfendazole is to be used in patients with neglected tropical infections in Sub-Saharan Africa, Southeast Asia, and South America, some differences in subjects' physical and health status might affect oxfendazole's exposure and response. For example, subjects in our study are primarily Caucasian, with an average weight of 82.4 kg, which is 32 to 55% higher than the average weight of adults in Africa and Southeast Asia (28). Another difference is with baseline hemoglobin concentrations. Patients in neglected tropical disease pandemic areas might have low baseline hemoglobin concentrations due to other conditions, such as malaria (29) or hookworm infection (30). In our study, oxfendazole appeared to have a mild suppressive effect on hemoglobin concentrations; therefore, attention to hemoglobin concentrations in future studies in patients is warranted.

In conclusion, we have developed a robust popPK/PD model that can adequately characterize oxfendazole pharmacokinetics, its effect on hemoglobin concentration in healthy adults following multiple ascending doses (3 to 15 mg/kg), and the effect of food on oxfendazole pharmacokinetics. The model was used to comprehensively evaluate the probability of target attainment of oxfendazole for whipworm infection and filariasis in human following various dose regimens and under different target attainment criteria. Due to the lack of available data on oxfendazole exposure-response in whipworm infection in human, results of target attainment analysis should be interpreted with caution. Nevertheless, the results of our modeling work, especially the target attainment analysis, are valuable for dose regimen selection in future trials in patient populations with different types of parasitic infections.

MATERIALS AND METHODS

Clinical data. The data used for popPK/PD model development come from the multiple ascending dose and food-effect study of oxfendazole in healthy adults that was published recently (23). Key information of the study is summarized below.

The study enrolled 36 subjects, 24 subjects in the multiple ascending dose evaluation and 11 subjects in the food-effect evaluation. Subject demographics are summarized in Table S1 in the supplemental material. Overall, demographic and baseline characteristics were similar across dose groups and dosing conditions. In the multiple ascending dose evaluation, subjects were randomized into three groups (8 subjects/group) corresponding to oxfendazole doses of 3, 7.5, and 15 mg/kg. Oxfendazole was administered as an oral suspension in a fasted state once daily for 5 days. Blood samples for pharmacokinetics assessment were collected on day 1 at predose and at 0.5, 1, 2, 3, 4, 6, 9, and 12 h postdose. On day 2, 3, and 4, samples were collected predose and at 2 h postdose. Samples were collected at 0, 0.5, 1, 2, 3, 4, 6, 9, 12, 24, 72, and 120 h after the last dose. Blood samples for safety assessment including hematology, biochemistry, and coagulation studies were collected at predose on day 1, 3, and 5 and at 72 h and 120 h after the last dose.

The food-effect evaluation adopted a randomized two-period (separated by 7 days) crossover study design with subjects taking a single oral dose of oxfendazole at 3 mg/kg following an overnight fast or a high-fat breakfast. Blood samples for oxfendazole quantification were collected at predose and at 0.5, 1, 2, 3, 4, 5, 6, 9, 12, and 24 h after each dose, and one sample was collected from each subject on day 14. For safety assessment, blood samples were collected at predose, day 4, and day 14.

The oxfendazole concentration in plasma was quantified using a validated liquid chromatography-tandem mass spectrometry assay with a linear range of 0.5 to 1,000 ng/ml (31). Intraday and interday accuracy of the quantitative method was in the range of 106.9 to 109.5%, and the coefficient of variability was no greater than 13.6% (31). Samples above the upper limit of quantification were diluted appropriately with blank human plasma (31). All samples were analyzed within the previously established stability time frame.

In total, 648 and 252 pharmacokinetics samples were collected and analyzed for the multiple ascending dose evaluation and the food-effect evaluation, respectively. Seven samples were disregarded due to sample misidentification. One hundred twenty samples from the multiple ascending dose study and 36 samples from the food-effect study were collected and analyzed for safety assessment. There was no drug-related change in any of the safety parameters except for hemoglobin concentrations in subjects in the multiple ascending dose study (23). Therefore, only hemoglobin concentrations from subjects in the multiple ascending dose evaluation were included in the popPK/PD model.

Population pharmacokinetic-pharmacodynamic development. NONMEM 7.4.0 (Icon Development, Ellicott City, MD, USA) with stochastic approximation expectation-maximization (SAEM) method and ADVAN13 subroutine was employed for nonlinear mixed-effect modeling. Visual predictive checks were performed using Perl-speaks-NONMEM (PsN) 4.8.0 (Uppsala Pharmacometrics Group) interfaced with Pirana 2.9.9 (Certara, Princeton, NJ, USA). R 4.0.2 (R Core Team) and RStudio 1.4.1103 (RStudio, PBC, Boston, MA, USA) were used for data processing and visualization.

(i) Handling of missing and BLQ data. Less than 2% of clinical samples (14 out of 893 samples) had a concentration below the limit of quantification (BLQ). Because the number of BLQ samples was low and all BLQ samples was collected after 120 h (i.e., more than 5 half-lives of oxfendazole), BLQ data were omitted from the popPK/PD analysis.

(ii) Structural model. Structural pharmacokinetic and pharmacodynamic models were developed sequentially.

(a) Pharmacokinetic model. The structural pharmacokinetic model for oxfendazole and metabolites in healthy adults following the administration of single ascending doses published previously (32) was adopted as the starting model. This model consisted of a depot compartment and a distribution compartment with first-order absorption and elimination. Because oxfendazole is a BCS class II drug with low solubility, the drug's bioavailability decreases with increasing dose, which resulted in a less than dose-proportional increase in exposure following ascending doses. Additionally, when oxfendazole was administered following a high fat meal, the bioavailability was increased. Consequently, oxfendazole bioavailability (F) was modeling using the following equation:

$$\log(F) = \theta_1 \log\left(\frac{\text{Dose}}{\theta_2}\right) + (\text{fast} - 1)\log(\theta_3) \tag{1}$$

where fast = 0 if oxfendazole is administered in the fasted state; otherwise, fast = 1.

According to equation 1, in the fasted state

$$\log(F_{\text{fast}}) = \theta_1 \log\left(\frac{\text{Dose}}{\theta_2}\right) - \log(\theta_3) \tag{2}$$

and in the fed state

$$\log(F_{\text{fed}}) = \theta_1 \log\left(\frac{\text{Dose}}{\theta_2}\right) \tag{3}$$

Therefore,

$$\log\left(\frac{F_{\text{fed}}}{F_{\text{fast}}}\right) = \log(F_{\text{fed}}) - \log(F_{\text{fast}}) = \log(\theta_3) \tag{4}$$

Thus,

$$\theta_3 = \frac{F_{\text{fed}}}{F_{\text{fast}}} \tag{5}$$

To simplify parameter estimation, it was assumed that $F = 1$ at the lowest dose in the fed state. Thus, θ_2 was fixed to 209.25 mg (corresponding to 3-mg/kg dose in a subject weighing 69.8 kg).

To capture the prolonged absorption phase of oxfendazole following consumption of a fatty meal, absorption models with 1 and 2 transit compartments were examined.

(b) Pharmacodynamic model. Exploratory analysis was performed by plotting the observed oxfendazole concentrations versus the observed hemoglobin concentrations (Fig. S3). Based on Fig. S3, no direct relationship was observed between oxfendazole and hemoglobin concentrations. Because hemoglobin concentrations were lower following the administration of multiple higher oxfendazole doses, indirect response models with either inhibition of hemoglobin synthesis or stimulation of hemoglobin elimination are plausible. Since oxfendazole inhibits tubulin assembly (33), oxfendazole has a suppressive effect on progenitor cells undergoing extensive cell division in the bone marrow, making more likely indirect response models with oxfendazole reducing hemoglobin synthesis. Two indirect response models of the inhibition of hemoglobin

synthesis were evaluated: the basic indirect response model and the life span indirect response model incorporating red blood cell life span.

In the basic indirect response model, the change in hemoglobin concentration (C_{Hb}) was modeled using the equation

$$\frac{dC_{Hb}}{dt} = k_{\text{in}} f(C_{\text{OXF}}(t)) - k_{\text{out}} C_{\text{OXF}} \tag{6}$$

where k_{in} is the red blood cell synthesis rate constant and k_{out} is the red blood cell elimination rate constant.

The change in hemoglobin concentration (C_{Hb}) in the life span model was modeled as

$$\frac{dC_{Hb}}{dt} = k_{in} f(C_{\text{OXF}}(t)) - k_{in} f(C_{\text{OXF}}(t - T_R)) \tag{7}$$

where T_R represents red blood cell life span and $f(C_{\text{OXF}}(t))$ is a function reflecting the inhibitory effect of oxfendazole concentration in the body at time t ($C_{\text{OXF}}(t)$). Linear and nonlinear correlations between oxfendazole concentration and oxfendazole inhibitory effect were evaluated. For linear correlation,

$$f(C_{\text{OXF}}(t)) = 1 - \theta \cdot C_{\text{OXF}}(t) \tag{8}$$

$$f(C_{\text{OXF}}(t - T_R)) = 1 - \theta \cdot C_{\text{OXF}}(t - T_R) \tag{9}$$

For nonlinear correlation,

$$f(C_{\text{OXF}}(t)) = 1 - \frac{I_{\max} C_{\text{OXF}}(t)}{\text{IC}_{50} + C_{\text{OXF}}(t)} \tag{10}$$

$$f(C_{\text{OXF}}(t - T_R)) = 1 - \frac{I_{\max} C_{\text{OXF}}(t - T_R)}{\text{IC}_{50} + C_{\text{OXF}}(t - T_R)} \tag{11}$$

where $I_{\max}$ is the maximal inhibitory effect, IC_{50} is oxfendazole concentration at 50% inhibition, $C_{\text{OXF}}(t)$ is oxfendazole concentration in the body at time t, and $C_{\text{OXF}}(t - T_R)$ is oxfendazole concentration in the body at time $t - T_R$.

(iii) Stochastic model. Interindividual variability and interoccasion variability were evaluated using the exponential model

$$P_i = TVP \cdot \exp\left(\eta_{i,0} + \text{OCC}_1 \cdot \eta_{i,1} + OCC_2 \cdot \eta_{i,2} \right) \tag{12}$$

where TVP represents the population mean of a pharmacokinetics or pharmacodynamic parameter, P_i represents the individual estimate of the corresponding parameter, $\eta_{i,0}$ represents interindividual variability, and $\eta_{i,1}$ and $\eta_{i,2}$ are interoccasion variabilities following the first and last doses. $OCC_1 = 1$ for the first dose; otherwise, $OCC_1 = 0$. $OCC_2 = 1$ for the last dose; otherwise, $OCC_2 = 0$. Interindividual variability and interoccasion variability are assumed to have a normal distribution with mean 0 and variance ω^2_{IIV} and ω^2_{IOV}, respectively.

For residual variability, an additive error model, a proportional error model, and a combined additive and proportional error model were examined. The following is an example of the combined additive and proportional error model.

$$C_{ij} = \overline{C_{ij}} \cdot (1 + \epsilon_{1ij}) + \epsilon_{2ij} \tag{13}$$

C_{ij} is the observed concentrations for individual i at time j, $\overline{C_{ij}}$ is the corresponding model predicted concentration, and ϵ_{1ij} and ϵ_{2ij} are proportional and additive errors, respectively. Additive and proportional residual variabilities were assumed to be normally distributed around 0 with variance of σ^2_1 and σ^2_2, respectively.

(iv) Covariate model. Initially, clinically meaningful covariates including sex, age, weight, body mass index (BMI), and creatinine clearance were plotted against interindividual variability of each pharmacokinetic and pharmacodynamic parameter. Potential covariates identified through graphical analysis were examined using stepwise forward addition and backward elimination. For stepwise forward addition, a decrease in objective function value (OFV) of more than 6.63 ($P < 0.01$) was considered significant improvement in model performance. For stepwise backward elimination, an increase in OFV of more than 10.83 ($P < 0.001$) was considered significant deterioration in model performance. The effects of continuous variables (i.e., age, weight, BMI, and creatinine clearance) were evaluated using the following general equation:

$$TVP_i = TVP\left(\frac{cov_i}{cov_m}\right)^{\theta_{cov}} \tag{14}$$

where TVP_i is the individual PK/PD parameter, TVP is the population mean of the corresponding PK/PD parameter, cov_i is the individual covariate, cov_m is the population mean of the covariate, and θ_{cov} is the covariate effect.

The effect of sex, a categorical variable, was assessed using the equation

$$TVP_i = TVP_{\text{male}} \cdot (\theta_{\text{sex}})^{\text{Sex}} \quad (15)$$

where TVP_{male} is the value of the PK/PD parameter in males. Sex = 1 for females and 0 for males. Thus, θ_{sex} is the ratio of a PK/PD parameter in females over that in males.

(v) Model evaluation. Models were selected based on feasibility and precision of parameter estimates and goodness-of-fit plots, including the plots of (i) observed concentration versus population predicted concentration, (ii) observed concentration versus individual predicted concentration, (iii) conditional weighted residual (CWRES) versus population predicted concentration, and (iv) CWRES versus time. For a good model, all data points would scatter evenly around the identity line in the former two plots and around the zero line in the latter two plots. Nested models were compared based on the difference in OFV (ΔOFV). ΔOFV was assumed to have a χ^2 distribution, with the degree of freedom being the difference in the number of parameters between the two nested models. On this basis, the addition of one parameter to the model was considered significantly improved model performance if OFV decreased more than 6.63, corresponding to a P value of <0.01. For nonnested models, AIC was used. The model with a smaller AIC was considered better.

Model predictive performance was evaluated using prediction-corrected visual predictive check of 1,000 simulations. Model predictive performance was acceptable if the observed 5th, 50th, and 95th percentiles fall within the 95% confidence interval of the corresponding simulated percentiles.

Simulation. (i) Simulation of exposure-response on safety. The simulation of exposure-response on safety focused on the effect of administration of multiple ascending doses of oxfendazole at 3, 7.5, 15, 30, and 60 mg/kg once daily for 5 days on hemoglobin concentrations in healthy adults. A thousand subjects were simulated for each dose level, assuming a 1:1 ratio of female to male subjects. Oxfendazole was administered using weight-normalized dose, but oxfendazole bioavailability depends on the absolute dose present in the gastrointestinal tract; therefore, subject weight needs to be included in the simulation to convert from weight-normalized dose to absolute dose. Subject weight distribution was based on the observed weight of participants in the oxfendazole multiple ascending dose trial. Female weight was simulated based on a normal distribution of a mean of 77.4 kg and standard deviation of 14.2 kg. For males, the mean weight was 84.6 kg and standard deviation was 13.0 kg. The simulated hemoglobin concentrations obtained were viewed in light of standard normal sex specific hemoglobin ranges.

(ii) Simulation of exposure-response on efficacy. ***(a) Target attainment analysis for whipworm infection (1st approach).*** Factors determining the effect of oxfendazole on *Trichuris trichiura* (human whipworm) are largely unknown. To carry out target attainment analysis, several assumptions were made based on literature information as provided below.

In a drug disposition study by Hansen et al. (22), a single oral dose of oxfendazole at 5 mg/kg was administered to pigs infected with *T. suis*. Blood samples and large intestinal samples were collected from the pigs over 48 h for quantification of oxfendazole in pig plasma, whole cecal tissue, cecal mucosa, cecal content, and whipworm. This study found that the concentration of oxfendazole in pig plasma ($C_{\text{OXF,plasma}}$ [nmol/ml]) was closely associated with the concentration of oxfendazole in whipworm ($C_{\text{OXF,worm}}$ [nmol/g]). Since the porcine parasite *T. suis* and the human-infecting *T. trichiura* have very similar growth habits, the anterior of the worm penetrating into the intestinal mucosa, with the posterior of the parasite freely moving in the intestinal lumen (22, 34), the findings of the Hansen study (22) also are thought to be relevant for the human *T. trichiura* infection. Further, the relative exposure to oxfendazole and its metabolites (oxfendazole sulfone and fenbendazole) in pigs and in humans is similar (21, 22), suggesting that pig is a good model for oxfendazole disposition in human. Thus, the correlation between oxfendazole concentration in host plasma and in intestinal dwelling whipworm was assumed to be similar for humans and pigs.

We digitized the data reported by Hansen et al. (22) using Engauge Digitizer (35) and converted oxfendazole concentration in whipworm in nanomoles per gram to concentration in nanomoles per milliliter based on body density of nematodes derived using the formulas for nematode body weight and body volume proposed by Andrassy (36).

$$\text{weight}(\,\mu\text{g}) = \frac{\text{length}(\,\mu\text{m}) \times \left(\text{diameter}(\,\mu\text{m})\right)^2}{1.6 \times 10^{-6}} \quad (16)$$

$$\text{volume}\left(\,\mu\text{m}^3\right) = \frac{\text{length}(\,\mu\text{m}) \times \left(\text{diameter}(\,\mu\text{m})\right)^2}{1.7} \quad (17)$$

According to these equations, all nematodes have the same body density.

$$\text{density} = \frac{\text{weight}}{\text{volume}} = 1.0625 \times 10^{-6}\,\frac{\mu\text{g}}{\mu\text{m}^3} \quad (18)$$

Based on the digitized data, the ratio between oxfendazole concentration in worm and oxfendazole concentration in pig plasma was quite consistent over time, with an average value of $C_{\text{OXF,worm}}(\text{nmol/ml})/C_{\text{OXF,plasma}}(\text{nmol/ml}) = 3.29$.

The principle pharmacological activity of benzimidazoles, including oxfendazole, stems from their binding to tubulin, resulting in inhibition of tubulin assembly (33). The oxfendazole IC_{50} to *T. trichiura* tubulin is unknown. However, an *in vitro* experiment evaluating oxfendazole inhibitory effect on tubulin

extracted from *Ascaris galli* (roundworm in bird) reported an IC_{50} of 5 μM (~1,580 ng/ml) (37). Because *A. galli* and *T. trichiura* are both intestinal nematodes, it was speculated that the oxfendazole IC_{50} to *T. trichiura* tubulin and *A. galli* tubulin would be similar.

To summarize, *in vitro* and preclinical efficacy data were applied to target attainment analysis for the treatment of whipworm infection in human based on the following assumptions: assumption 1, $C_{OXF,worm}(nmol/ml)/C_{OXF,plasma}(nmol/ml) = 3.29$; assumption 2, oxfendazole IC_{50} to whipworm tubulin and *A. galli* tubulin is the same and is equivalent to 1580 ng/ml; assumption 3, the worm body is a well-stirred model.

Based on these assumptions, an oxfendazole IC_{50} of 1,580 ng/ml at the site of tubulin assembly corresponds to an oxfendazole concentration of 480 ng/ml in human plasma.

Oxfendazole concentration-time profiles were simulated following the administration of multiple ascending oxfendazole doses of 0.5 to 60 mg/kg once daily for 5 days, with 1,000 subjects at each dose. Subject sex and weight distribution was the same as in the safety simulation. Because it is unknown whether the antiparasitic efficacy of oxfendazole depends on the achievement of an effective concentration or the maintenance over some time period of the effective concentration, two scenarios were investigated. In the first scenario, oxfendazole antiparasitic efficacy was assumed to be dependent on attainment of a targeted $C_{max,ss}$. The range of targeted $C_{max,ss}$ evaluated was 1 to 40 times the IC_{50} (480 ng/ml). In the second scenario, oxfendazole antiparasitic efficacy was assumed to be dependent on maintenance of the oxfendazole concentration above the IC_{50} for a certain amount of time, as reflected by the percent time dosing interval (24 h) at steady state during which the oxfendazole concentration is above IC_{50} ($T_{>IC50}$). Ranges of $T_{>IC50}$ explored included <40%, 40 to <60%, 60 to <80%, 80 to <100%, and 100%. The probability of target attainment is the percentage of simulated subjects being able to attain the targeted $C_{max,ss}$ or $T_{>IC50}$.

(b) Target attainment analysis for whipworm infection (2nd approach). A recent study by Keiser and Haberli evaluated the survival of *Trichuris muris* (whipworm collected from rodents) in culture in the presence of various antiparasitic drugs (26). Whipworm survival was assessed based on whipworm motility. This study reported an IC_{50} of 55.2 μM (~17,405 ng/ml) for oxfendazole (26). To utilize this information for target attainment analysis, the following assumptions were made: assumption 1, $C_{OXF,worm}/C_{OXF,plasma} = 3.29$; assumption 2, oxfendazole IC_{50} is the same for *T. muris* and *T. trichiura*.

Based on these assumptions, an oxfendazole IC_{50} of 17,405 ng/ml to *T. trichiura* was translated to 5,290 ng/ml in human plasma. Two target attainment analyses were carried out, one evaluating $C_{max,ss}$ and the other evaluating $T_{>IC50}$, as described for the 1st approach.

(c) Target attainment analysis for filariasis. To evaluate the macrofilaricidal efficacy of oxfendazole, Hubner et al. utilized *Litomosoides sigmodontis*-infected mice, a surrogate model for filariasis in human (13). Oxfendazole was administered to infected mice orally or subcutaneously once daily or twice daily for 1, 5, or 10 days at doses ranging from 1 to 125 mg/kg per day. Macrofilaricidal efficacy was assessed by adult worm count. The study showed that sterile cure was achieved with an oral dose of 12.5 mg/kg twice daily for 5 days or subcutaneous dose of 25 mg/kg once daily for 5 days (13). Concurrently, oxfendazole pharmacokinetics following the administration of a single subcutaneous dose of 1 and 25 mg/kg or a single oral dose of 5 or 25 mg/kg was evaluated in a parallel untreated group of mice (13). Based on their efficacy and pharmacokinetic results, Hubner et al. suggested that oxfendazole macrofilaricidal efficacy is driven by the maintenance of its MEC in plasma above 100 ng/ml (13). Thus, for target attainment analysis, the percentage of the simulated population with oxfendazole concentration at steady state being equal to or greater than the MEC was computed. To account for the uncertainty of extrapolating data from mice to humans, a range of MEC from 100 to 4,000 ng/ml was investigated in the present study.

SUPPLEMENTAL MATERIAL

Supplemental material is available online only.

SUPPLEMENTAL FILE 1, PDF file, 1.1 MB.

ACKNOWLEDGMENTS

This work was supported by the Division of Microbiology and Infectious Diseases, National Institute of Allergy and Infectious Diseases, National Institutes of Health, through the Vaccine and Treatment Evaluation Unit (contract no. HHSN272200800008C and HHSN24220130020I) and by the National Center for Advancing Translational Sciences grant to the University of Iowa (grant no. 5U54TR001356) for the work done in the Clinical Research Unit.

REFERENCES

1. WHO. 2020. Ending the neglect to attain the sustainable development goals–a roadmap for the neglected tropical diseases 2021–2030. https://www.who.int/neglected_diseases/Ending-the-neglect-to-attain-the-SDGs-NTD-Roadmap.pdf. Accessed 2 February 2021.
2. Garcia HH, Gilman RH, Horton J, Martinez M, Herrera G, Altamirano J, Cuba JM, Rios-Saavedra N, Verastegui M, Boero J, Gonzalez AE. 1997. Albendazole therapy for neurocysticercosis: a prospective double-blind trial comparing 7 versus 14 days of treatment. Cysticercosis Working Group in Peru. Neurology 48:1421–1427. https://doi.org/10.1212/wnl.48.5.1421.
3. Moser W, Schindler C, Keiser J. 2017. Efficacy of recommended drugs against soil transmitted helminths: systematic review and network meta-analysis. BMJ 358:j4307. https://doi.org/10.1136/bmj.j4307.
4. Mihmanli M, Idiz UO, Kaya C, Demir U, Bostanci O, Omeroglu S, Bozkurt E. 2016. Current status of diagnosis and treatment of hepatic echinococcosis. World J Hepatol 8:1169–1181. https://doi.org/10.4254/wjh.v8.i28.1169.
5. Katiyar D, Singh LK. 2011. Filariasis: current status, treatment and recent advances in drug development. Curr Med Chem 18:2174–2185. https://doi.org/10.2174/092986711795656234.

6. Caravedo MA, Cabada MM. 2020. Human fascioliasis: current epidemiological status and strategies for diagnosis, treatment, and control. Res Rep Trop Med 11:149–158. https://doi.org/10.2147/RRTM.S237461.
7. Dawson M, Allan RJ, Watson TR. 1982. The pharmacokinetics and bioavailability of mebendazole in man: a pilot study using [3H]-mebendazole. Br J Clin Pharmacol 14:453–455. https://doi.org/10.1111/j.1365-2125.1982.tb02008.x.
8. Dawson M, Braithwaite PA, Roberts MS, Watson TR. 1985. The pharmacokinetics and bioavailability of a tracer dose of [3H]-mebendazole in man. Br J Clin Pharmacol 19:79–86. https://doi.org/10.1111/j.1365-2125.1985.tb02616.x.
9. Corti N, Heck A, Rentsch K, Zingg W, Jetter A, Stieger B, Pauli-Magnus C. 2009. Effect of ritonavir on the pharmacokinetics of the benzimidazoles albendazole and mebendazole: an interaction study in healthy volunteers. Eur J Clin Pharmacol 65:999–1006. https://doi.org/10.1007/s00228-009-0683-y.
10. Anonymous. 1990. Freedom of information summary, NADA 140–854 synanthic-original approval. https://animaldrugsatfda.fda.gov/adafda/app/search/public/document/downloadFoi/505.
11. Alvarez L, Saumell C, Fuse L, Moreno L, Ceballos L, Domingue G, Donadeu M, Dungu B, Lanusse C. 2013. Efficacy of a single high oxfendazole dose against gastrointestinal nematodes in naturally infected pigs. Vet Parasitol 194:70–74. https://doi.org/10.1016/j.vetpar.2013.01.003.
12. Corwin RM, Kennedy JA, Pratt SE. 1979. Dose titration of oxfendazole against common nematodes of swine. Am J Vet Res 40:297–298.
13. Hubner MP, Martin C, Specht S, Koschel M, Dubben B, Frohberger SJ, Ehrens A, Fendler M, Struever D, Mitre E, Vallarino-Lhermitte N, Gokool S, Lustigman S, Schneider M, Townson S, Hoerauf A, Scandale I. 2020. Oxfendazole mediates macrofilaricidal efficacy against the filarial nematode Litomosoides sigmodontis in vivo and inhibits Onchocerca spec. motility in vitro. PLoS Negl Trop Dis 14:e0008427. https://doi.org/10.1371/journal.pntd.0008427.
14. Gonzalez AE, Codd EE, Horton J, Garcia HH, Gilman RH. 2019. Oxfendazole: a promising agent for the treatment and control of helminth infections in humans. Expert Rev Anti Infect Ther 17:51–56. https://doi.org/10.1080/14787210.2018.1555241.
15. Codd EE, Ng HH, McFarlane C, Riccio ES, Doppalapudi R, Mirsalis JC, Horton RJ, Gonzalez AE, Garcia HH, Gilman RH, Cysticercosis Working Group in Peru. 2015. Preclinical studies on the pharmacokinetics, safety, and toxicology of oxfendazole: toward first in human studies. Int J Toxicol 34:129–137. https://doi.org/10.1177/1091581815569582.
16. Gokbulut C, Bilgili A, Hanedan B, McKellar QA. 2007. Comparative plasma disposition of fenbendazole, oxfendazole and albendazole in dogs. Vet Parasitol 148:279–287. https://doi.org/10.1016/j.vetpar.2007.06.028.
17. Lanusse CE, Gascon LH, Prichard RK. 1995. Comparative plasma disposition kinetics of albendazole, fenbendazole, oxfendazole and their metabolites in adult sheep. J Vet Pharmacol Ther 18:196–203. https://doi.org/10.1111/j.1365-2885.1995.tb00578.x.
18. Moreno L, Lopez-Urbina MT, Farias C, Domingue G, Donadeu M, Dungu B, Garcia HH, Gomez-Puerta LA, Lanusse C, Gonzalez AE. 2012. A high oxfendazole dose to control porcine cysticercosis: pharmacokinetics and tissue residue profiles. Food Chem Toxicol 50:3819–3825. https://doi.org/10.1016/j.fct.2012.07.023.
19. Alvarez LI, Saumell CA, Sanchez SF, Lanusse CE. 1996. Plasma disposition kinetics of albendazole metabolites in pigs fed different diets. Res Vet Sci 60:152–156. https://doi.org/10.1016/S0034-5288(96)90010-7.
20. Allan RJ, Watson TR. 1983. The metabolic and pharmacokinetic disposition of mebendazole in the rat. Eur J Drug Metab Pharmacokinet 8:373–381. https://doi.org/10.1007/BF03188769.
21. An G, Murry DJ, Gajurel K, Bach T, Deye G, Stebounova LV, Codd EE, Horton J, Gonzalez AE, Garcia HH, Ince D, Hodgson-Zingman D, Nomicos EYH, Conrad T, Kennedy J, Jones W, Gilman RH, Winokur P. 2019. Pharmacokinetics, safety, and tolerability of oxfendazole in healthy volunteers: a randomized, placebo-controlled first-in-human single-dose escalation study. Antimicrob Agents Chemother 63:e02255-18. https://doi.org/10.1128/AAC.02255-18.
22. Hansen TVA, Williams AR, Denwood M, Nejsum P, Thamsborg SM, Friis C. 2017. Pathway of oxfendazole from the host into the worm: trichuris suis in pigs. Int J Parasitol Drugs Drug Resist 7:416–424. https://doi.org/10.1016/j.ijpddr.2017.11.002.
23. Bach T, Galbiati S, Kennedy JK, Deye G, Nomicos EYH, Codd EE, Garcia HH, Horton J, Gilman RH, Gonzalez AE, Winokur P, An G. 2020. Pharmacokinetics, safety, and tolerability of oxfendazole in healthy adults in an open label phase 1 multiple ascending dose and food effect study. Antimicrob Agents Chemother 64:e01018-20. https://doi.org/10.1128/AAC.01018-20.
24. Lange H, Eggers R, Bircher J. 1988. Increased systemic availability of albendazole when taken with a fatty meal. Eur J Clin Pharmacol 34:315–317. https://doi.org/10.1007/BF00540964.
25. Janssen. 2017. Mebendazole label. https://www.accessdata.fda.gov/drugsatfda_docs/label/2016/208398s000lbl.pdf. Accessed 26 January 2019.
26. Keiser J, Haberli C. 2021. Evaluation of commercially available anthelminthics in laboratory models of human intestinal nematode infections. ACS Infect Dis https://doi.org/10.1021/acsinfecdis.0c00719.
27. FAO. 1998. Residues of some veterinary drugs in foods and animals: 41–4-oxfendazole. http://www.fao.org/fileadmin/user_upload/vetdrug/docs/41-4-oxfendazole.pdf.
28. Hayes DJ, Buuren S, Ter Kuile FO, Stasinopoulos DM, Rigby RA, Terlouw DJ. 2015. Developing regional weight-for-age growth references for malaria-endemic countries to optimize age-based dosing of antimalarials. Bull World Health Organ 93:74–83. https://doi.org/10.2471/BLT.14.139113.
29. White NJ. 2018. Anaemia and malaria. Malar J 17:371. https://doi.org/10.1186/s12936-018-2509-9.
30. Layrisse M, Roche M. 1964. The relationship between anemia and hookworm infection. Results of surveys of rural Venezuelan population. Am J Hyg 79:279–301. https://doi.org/10.1093/oxfordjournals.aje.a120383.
31. Bach T, Bae S, D'Cunha R, Winokur P, An G. 2019. Development and validation of a simple, fast, and sensitive LC/MS/MS method for the quantification of oxfendazole in human plasma and its application to clinical pharmacokinetic study. J Pharm Biomed Anal 171:111–117. https://doi.org/10.1016/j.jpba.2019.03.048.
32. Bach T, Murry DJ, Stebounova LV, Deye G, Winokur P, An G. 2021. Population pharmacokinetic model of oxfendazole and metabolites in healthy adults following single ascending doses. Antimicrob Agents Chemother 65:e02129-20. https://doi.org/10.1128/AAC.02129-20.
33. McKellar QA, Scott EW. 1990. The benzimidazole anthelmintic agents–a review. J Vet Pharmacol Ther 13:223–247. https://doi.org/10.1111/j.1365-2885.1990.tb00773.x.
34. CDC. Trichuriasis. https://www.cdc.gov/parasites/whipworm/biology.html. Accessed 6 April 2021.
35. Mitchell M, Muftakhidinov B, Winchen T, Wilms A, Schaik B, Mo-Gul B, Badger TG, Jędrzejewski-Szmek Z, Kensington K. 2021. Engauge Digitizer software. https://markummitchell.github.io/engauge-digitizer/. Accessed 29 June 2021.
36. Andrassy I. 1956. Die rauminhalts-und gewichtsbestimmung der fadenwürmer (Nematoden). Acta Zool Hungarica 2:1–5.
37. Dawson PJ, Gutteridge WE, Gull K. 1984. A comparison of the interaction of anthelmintic benzimidazoles with tubulin isolated from mammalian tissue and the parasitic nematode Ascaridia galli. Biochem Pharmacol 33:1069–1074. https://doi.org/10.1016/0006-2952(84)90515-x.